17th Brazilian Congress of Thermal Sciences and Engineering
November 25th-28th, 2018, Águas de Lindóia, SP, Brazil

ENCIT-2018-0027
NUMERICAL STUDY OF A CAVITY WITH AND WITHOUT RADIATION INCLUDING A PARTICIPATING WET AIR

Ana Carolina Oliveira de Paula
Kamal Abdel Radi Ismail
University of Campinas, Faculty of Mechanical Engineering, Department of Energy, Rua Mendeleyev, 200, Cidade Universitária "Zeferino Vaz", Postal Code 13083-860, Campinas – SP, Brazil.
ana.carolina@fem.unicamp.br
kamal@fem.unicamp.br

Abstract. *The present paper numerically investigates heat transfer and fluid flow by binary natural convection and radiative heat transfer in an inclined solar still cavity filled with air and water vapor. A comparison is performed for a cavity where thermal radiation is included and one where it is not. For the radiative cavity, walls are considered surfaces that reflect and emit diffusively, while wet air is considered to be a participating medium. For the non-radiative cavity, radiative exchange at the walls and working fluid is not considered. Water vapor is at the saturation state. Conservative equations (mass, momentum, energy and species) are analyzed and discretized through control volume method (CVM). Velocity-pressure linkage is solved through the SIMPLE algorithm. Radiative transfer is solved using the discrete ordinates method (DOM) and is coupled in the energy equation. Velocity, temperature and concentration fields are obtained for a Rayleigh number range where laminar flow prevails. Results show that radiation heat transfer changes fluid dynamics inside the solar still cavity. Temperature and velocity contour lines tend to concentrate close to the wall of higher emissivity. Changes were also present in Nusselt number profiles, where peaks were observed in the regions close to the walls.*

Keywords: *solar still, binary natural convection, radiative transfer, discrete ordinates method*

1. INTRODUCTION

Binary natural convection is a phenomenon that exists in many engineering applications such as refrigeration towers, processes of pollutants dispersion, drying and solar distillation. One of the first numerical studies performed in the area of natural convection was elaborated by Davis (1983). The author published a numerical solution for a square cavity in which vertical walls were at different levels of temperature. The author published results for thermal Rayleigh number varying from 10^3 to 10^6 that are considered benchmark and have been used for validation of other numerical studies. Le Quéré (1991) proposed a numerical solution using pseudo-spectral discretization to provide accurate solutions for values of thermal Rayleigh number between 10^7 and 10^8, once the classical Boussinesq approximation becomes unsteady in this thermal Rayleigh number range.

Béghein et al. (1992) published a numerical study considering double-diffusion in a closed square cavity filled with air and pollutants. The authors compared the effects of thermal and solutal buoyancy forces through Nusselt and Sherwood numbers. Weaver and Viskanta (1992) elaborated a numerical-experimental study that could verify flow direction change when buoyancy parameters were reversed in direction. Seizai and Mohamad (2000) investigated a cubic cavity for opposing, horizontal, thermal and solutal gradients. It was found that secondary flow structures develop on the planes perpendicular to the main flow, especially for high Rayleigh number. Paula and Ismail (2017) published results for binary natural convection in an inclined cavity and concluded that Nusselt and Sherwood numbers peaks exist at the hot wall in the regions of high gradients of temperature, concentration and velocities.

Most part of the published studies do not consider the radiative effects of the cavity walls and medium in order to avoid computational effort. Most part of published works that consider radiative transfer only account to the effects of cavity walls because most of main gases, such as O_2, N_2 and H_2 are almost transparent to thermal radiation. Akiyama and Chong (1997) published results for the interaction of natural convection and surface thermal radiation of a cavity filled with air. Authors compared Nusselt Number variations when thermal Rayleigh number and wall emissivity were changed. According to Lari, *et al*., (2011), the effect of participating gases cannot be ignored even at ambient temperature. In their study, the coupling between natural convection and radiative heat transfer was performed for a two-dimensional black walls cavity and medium that emits and absorbs. It was verified that, for a transparent medium, radiation is the dominant mean of heat exchange. However, this contribution tends to decrease when gas optical thickness is increased. Performance of different RTE solvers were tested by Sun, *et al*., (2017), where the discrete ordinates method (DOM) proved to be the most accurate and efficient method for coupled natural convection and radiation heat transfer problems.

The present paper numerically investigates the effects of coupling binary natural convection and radiative heat transfer in a solar still cavity. The cavity is inclined and contains two adiabatic and impermeable walls and two walls subject to temperature and water vapor concentration gradients. The cavity walls are surfaces that reflect and emit diffusively, while wet air is considered to be a participating medium approximated as a gray gas. The cavity performance is evaluated through heat and mass transfer parameters (Nusselt and Sherwood numbers) for different values of Rayleigh number that represent laminar regime. Temperature difference is considered low, thus, Boussinesq approach is applied along with constant thermophysical properties.

2. ANALYSIS

Figure 1 presents the two-dimensional inclined solar still cavity. The cavity contains two insulating and impermeable walls and two walls at different levels of temperature and water vapor concentration. The temperature and concentration at the bottom are slightly higher than upper surface. Vapor is formed at saturate state at bottom wall and condenses out of the mixture at the top wall. The condensed water is free of particulate (salts) and slides along the glass because of cavity inclination.

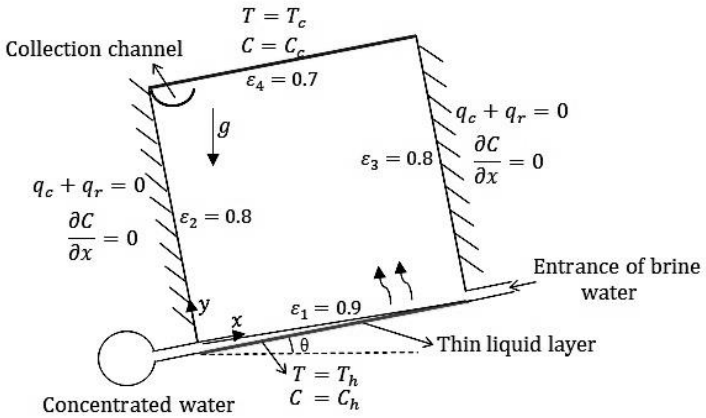

Figure 1. Solar still cavity

The representation of fluid dynamics, heat and mass transfer in the cavity is obtained considering the following conservation equations:

$$\frac{\partial \rho}{\partial t} + \frac{\partial (\rho u)}{\partial x} + \frac{\partial (\rho v)}{\partial y} = 0 \tag{1}$$

$$-\frac{\partial p}{\partial x} + \mu\left(\frac{\partial^2 u}{\partial x^2} + \frac{\partial^2 u}{\partial y^2}\right) + (\rho - \rho_{ref})\, g \sin(\theta) = \frac{\partial (u\rho)}{\partial t} + \frac{\partial (\rho u \cdot u)}{\partial x} + \frac{\partial (\rho v \cdot u)}{\partial y} \tag{2}$$

$$-\frac{\partial p}{\partial y} + \mu\left(\frac{\partial^2 v}{\partial x^2} + \frac{\partial^2 v}{\partial y^2}\right) + (\rho - \rho_{ref})\, g \cos(\theta) = \frac{\partial (v\rho)}{\partial t} + \frac{\partial (\rho u \cdot v)}{\partial x} + \frac{\partial (\rho v \cdot v)}{\partial y} \tag{3}$$

$$\frac{\partial (\rho T)}{\partial t} + \frac{\partial (\rho u \cdot T)}{\partial x} + \frac{\partial (\rho v \cdot T)}{\partial y} = \frac{k}{c_p}\left(\frac{\partial^2 T}{\partial x^2} + \frac{\partial^2 T}{\partial y^2}\right) - \frac{1}{c_p}\nabla q_r \tag{4}$$

$$D_v\left(\frac{\partial^2 C_v}{\partial x^2} + \frac{\partial^2 C_v}{\partial y^2}\right) = \frac{\partial (C_v)}{\partial t} + \frac{\partial (u \cdot C_v)}{\partial x} + \frac{\partial (v \cdot C_v)}{\partial y} \tag{5}$$

where ρ corresponds the density of main species (air), u and v corresponds to velocities in x and y directions respectively, and p is the pressure acting in the corresponding control volume. The reference density is ρ_{ref} (density at the reference temperature T_{ref}), g is the gravitational acceleration, μ is the dynamic viscosity of air, k is the air thermal conductivity and c_p is the air specific heat. The binary diffusive coefficient is given by D_v and C_v is the concentration of the water vapor. The reference temperature (T_{ref}) and concentration (C_{ref}) are given by (T_h + T_c)/2 and (C_h + C_c)/2

respectively, where T_h, C_h, T_c and C_c are the temperatures and concentrations at hot and cold wall. The buoyancy term is evaluated by Boussinesq approximation:

$$\left(\rho - \rho_{ref}\right) = \rho\beta_T\left(T_{ref} - T\right) + \rho\beta_S\left(C_{ref} - C\right) \tag{6}$$

where β_T and β_S are the thermal and solutal expansion coefficients respectively. These coefficients are given by Jabrallah, *et al.*, (2002):

$$\beta_T = -\frac{1}{\rho}\left(\frac{\partial\rho}{\partial T}\right)_P = \frac{1}{T_{ref}} \tag{7}$$

$$\beta_S = -\frac{1}{\rho}\left(\frac{\partial\rho}{\partial C}\right)_{P,T} = \frac{M_a - M_v}{C_v M_v + C_a M_a} \tag{8}$$

The divergence of radiative flux is given by:

$$\nabla \cdot q_r = \kappa_n\left(4\pi I_{bn}(r) - \int_{4\pi} I(r,\Omega)\,d\Omega\right) \tag{9}$$

where κ_n is the spectral absorption coefficient, I is radiation intensity and I_{bn} is the spectral radiation intensity of black body. To obtain the divergence of radiative flux, it is necessary to solve the radiative transfer equation (RTE):

$$(\Omega \cdot \nabla) I(r,\Omega) = -\beta_n I(r,\Omega) + \kappa_n I_{bn}(r) + \frac{\sigma_s}{4\pi}\int_{4\pi} I(r,\Omega')\,d\Omega' \tag{10}$$

where σ_s is the scattering coefficient and β_n is the extinction coefficient ($\beta_n = \kappa_n + \sigma_s$). For air-water vapor mixture, scattering is not present, thus, the last term of Eq. (10) is despised. Also, at this stage, optical properties of the participating gas are considered constant over spectral lines (gray gas approximation). Optical thickness and linear absorption coefficient are related by:

$$\tau_n = \int_0^s \beta_n\,ds \tag{11}$$

where s is the direction of propagation. The surface radiative flux is obtained by:

$$q_r = \varepsilon_n\left(\pi I_{bn}(r_w) - \int_{n.\Omega'<0} I(r_w,\Omega')\left|n.\Omega'\right|d\Omega'\right) \tag{12}$$

where ε_n is the surface emissivity. For opaque, diffusively emissive and reflective walls:

$$I(r_w,\Omega) = \varepsilon_n I_{bn}(r_w) + \frac{(1-\varepsilon_n)}{\pi}\int_{n.\Omega'<0} I(r_w,\Omega')\left|n.\Omega'\right|d\Omega' \tag{13}$$

The difference between hot and cold wall is defined by the non-dimensional temperature parameter $\in$. Thermal and solutal Rayleigh numbers are defined as:

$$Ra_T = g\beta_T\left(T_h - T_c\right)H^3 / \nu\alpha \tag{14}$$

$$Ra_S = g\beta_S\left(C_h - C_c\right)H^3 / \nu D_v \tag{15}$$

where ν is the kinematic viscosity of the main species (air). Prandtl and Lewis number are defined:

$$\mathrm{Pr} = \nu / \alpha \tag{16}$$

$$Le = \alpha / D_v \tag{17}$$

Convective, radiative and overall Nusselt numbers at the walls are respectively calculated by:

$$Nu = \frac{q_c H}{k\Delta T} \tag{18}$$

$$Nu_r = \frac{q_r H}{k\Delta T} \tag{19}$$

$$Nu_T = Nu + Nu_r \tag{20}$$

where q_c is the convective heat flux and q_r radiative heat flux. Finally, Sherwood number is evaluated by the expression:

$$Sh = \frac{\dot{m}_v H}{D_v \Delta C_v} \tag{21}$$

where m_v is the vapor flux being transferred by convection.

2.1 Boundary conditions

The domain of the problem consists of a square cavity ($0 \leq x \leq H$ and $0 \leq y \leq H$) in which binary natural convection takes place due to temperature and vapor concentration difference. Inclination angle is θ = 25°. The reference temperature is T_{ref} = 320 K and non-dimensional temperature difference is defined to be $\in$ = 0.05. Therefore, Boussinesq limits are not extrapolated. Top wall is subject to $T_c = T_{ref}$ (1–$\in$) and bottom wall is subject to $T_h = T_{ref}$ (1+$\in$). Vertical walls are adiabatic and impermeable. Vapor concentration at the walls can be obtained through the state equation for an ideal gas:

$$C_h = p_{sat}(T_h) / \Re T_h \tag{22}$$

$$C_c = p_{sat}(T_c) / \Re T_c \tag{23}$$

where $\Re$ is the universal constant of gases. Walls are considered to be surfaces that emit and reflect thermal radiation diffusely (ε_1 = 0.9, ε_2 = 0.8, ε_3 = 0.8 and ε_4 = 0.7). Mixture of air and water vapor is considered to be a participating medium. At this stage, optical properties of the participating gas are considered constant over spectral lines (gray gas approximation). Once air is the predominant gas in the cavity (representing over 95% of the mixture), maximum average optical thickness for the air is about τ_n = 0.1, as mentioned by Lari, *et al.*, (2011). Thus, this value is used for gas optical thickness. Gas extinction coefficient is determined according to Eq. (11). Thermophysical properties considered in the domain are taken at the reference temperature: k=2.78 W/mK, c_p=1.006·10^3 J/kgK, ρ=1.0948 kg/m^3, Pr=0.71 and D_v=0.29·10^{-4} m^2/s.

3. NUMERICAL TREATMENT

The numerical solution strategy initiates with conservation equations (1-5) discretization through finite volume method. Velocity-pressure coupling is solved using SIMPLE algorithm (abbreviation for Semi-Implicit Method for Pressure-Linked Equations), as presented by Patankar (1980). Convective terms are approximated using hybrid scheme while diffusive terms are approximated by central difference. Fully implicit scheme is used for time discretization. False transient formulation and variable under-relaxation were used in order to improve convergence. Scalar variables are calculated in a 61x61 main grid, while velocity components are calculated in a staggered grid. Both grids are refined near the walls using a hyperbolic transformation function presented by Sengupta, *et al.*, (2011). The divergent of radiative flux in energy equation is calculated solving RTE and is considered as a source term of the energy equation. RTE is spatially discretized by the finite volume method and directionally discretized through the discrete ordinates method (DOM). In this sense, RTE is substituted by a set of m = 1,…,M discrete directions, as follows:

$$\xi_m \left(A_E I_E^m - A_W I_W^m \right) + \eta_m \left(A_N I_N^m - A_S I_S^m \right) = -\beta_n I_p{}^m V_p + \kappa_n I_{bn,p}^m V_p \tag{24}$$

By linear interpolation, $I_p{}^m$ can be expressed by:

$$I_p^m = \varsigma I_E^m + (1-\varsigma) I_W^m = \varsigma I_S^m + (1-\varsigma) I_S^m \tag{25}$$

Substituting in Eq. (24), the obtained expression for I_p^m is:

$$I_p^m = \frac{|\xi|\Delta y I_W^m + |\eta|\Delta x I_S^m + \varsigma \kappa_n I_{bn,p}^m V_p}{|\xi|\Delta y + |\eta|\Delta x + \varsigma \beta_n V_p} \tag{26}$$

Step scheme is used for linear interpolation (ς = 1). Applying DOM in the boundary conditions we obtain:

$$I(r_w, \Omega_m) = \varepsilon I_{bn}(r_w) + \frac{(1-\varepsilon_n)}{\pi} \sum_{\substack{m=1 \\ n.\Omega'<0}}^{M/2} w_k I(r_w, \Omega_k) |n.\Omega'| \tag{27}$$

3.1 Validation of code and verifications

Validation of numerical code was done for two main analyses: binary natural convection and combined natural convection and radiative heat transfer. For binary natural convection validation, the results were compared to the benchmark paper published by Béghein, *et al.*, (1992) for a cavity with temperature and species concentration difference between vertical walls, for $Ra_T = 10^4$ and $Ra_S = 10^4$ (validation results are presented in Fig. 2). Natural convection and thermal radiation coupling was validated for a differentially heated cavity with black walls (ε = 1) filled with air. In this situation, vertical walls were at different level of temperatures. Results were compared to the ones published by Lari, *et al.*, (2011) for $Ra_T = 10^5$ and 10^6 and different optical thickness (τ = 0, 1 and 5), as presented in Table 1. In parenthesis, relative errors are shown.

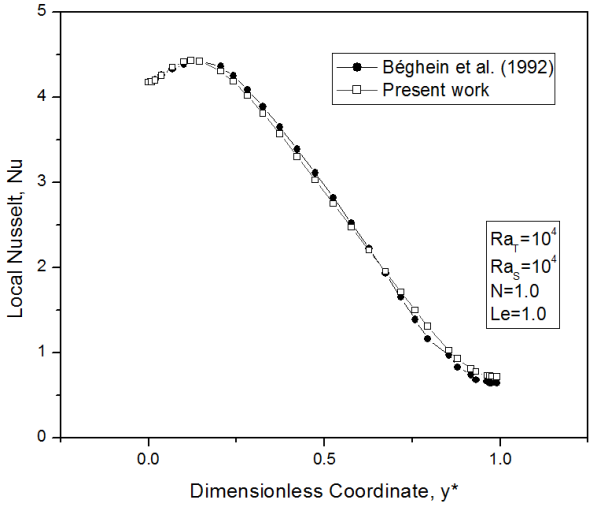

Figure 2. Comparison of local Nusselt number along the hot wall of an enclosed cavity

Table 1: Comparison of total Nusselt numbers at the hot wall for different optical thicknesses.

Nu_T	$Ra_T = 10^5$			$Ra_T = 10^6$		
	$\tau = 0$	$\tau = 1$	$\tau = 5$	$\tau = 0$	$\tau = 1$	$\tau = 5$
Lari, *et al.*, (2011)	10.118	8.349	6.776	20.667	17.120	14.462
Present work	10.217 (0.9%)	8.355 (0.07%)	6.775 (0.01%)	20.917 (1,2%)	17.146 (0.15%)	14.512 (0.3%)

Sensitivity analysis is performed to check grid and angular quadrature independency. Analyzes are performed for the solar still problem. Table 2 shows results for overall Nusselt number at the bottom wall (hot wall) for 41x41, 51x51 and 61x61 grid numbers using S_4 angular quadrature. Results indicate that the difference between grids is small. Table 3 shows results for overall Nusselt number at the bottom wall (hot wall) for S_4 and S_8 quadratures, directions obtained from Modest (2013). Aiming to obtain accurate results, 61x61 grid and S_8 quadrature is chosen for the following analyzes.

Table 2: Comparison of total Nusselt numbers at the hot wall for different grid numbers.

Nu_T	$Ra_T = 10^3$	$Ra_T = 10^4$	$Ra_T = 10^5$	$Ra_T = 10^6$
41x41	6.172	13.050	26.723	54.943
51x51	6.167	13.051	26.706	54.883
61x61	6.164	13.049	26.691	54.837

Table 3: Comparison of total Nusselt numbers at the hot wall for different quadratures.

Nu_T	$Ra_T = 10^3$	$Ra_T = 10^4$	$Ra_T = 10^5$	$Ra_T = 10^6$
S_4	6.164	13.049	26.691	54.837
S_8	6.181	13.056	26.664	54.717

4. RESULTS AND DISCUSSION

This section discusses the numerical solutions and results for heat and mass transfer inside a solar still cavity subject to temperature and species concentration gradients. Cavity walls are surfaces that emit and reflect thermal radiation. Air and water vapor mixture is considered to be a participating medium. Optical properties of the participating gas are considered constant over the spectrum (gray gas approximation). In this study, analysis will be performed for thermal Rayleigh number between 10^3 and 10^6 to ensure laminar flow. In order to obtain the desired Rayleigh values, the cavity height was varied. Consequently, absorption of the medium also changed according to Eq. (11). The cavity equivalent dimensions are presented in Table 4.

Table 4: Cavity equivalent dimensions

	$Ra_T = 10^3$	$Ra_T = 10^4$	$Ra_T = 10^5$	$Ra_T = 10^6$
H (m)	0.008	0.017	0.037	0.077

Figures 3, 4 and 5 present results for temperature, velocities and vapor concentration fields for the case where thermal radiation is included (radiative case) and the case where thermal radiation was not included (non-radiative case). Results indicate that the consideration of radiation exchange in the model significantly changed heat and mass transfer inside solar still cavity. Temperature contour lines presented great changes in the considered thermal Rayleigh number range. Isotherms concentrate mostly at the bottom wall because the emissivity at this wall is the highest. Top wall presented the lowest emissivity, and for this reason, held low isotherms concentration. Velocity and concentration fields also presented changes. These changes can be better noticed for high thermal Rayleigh number.

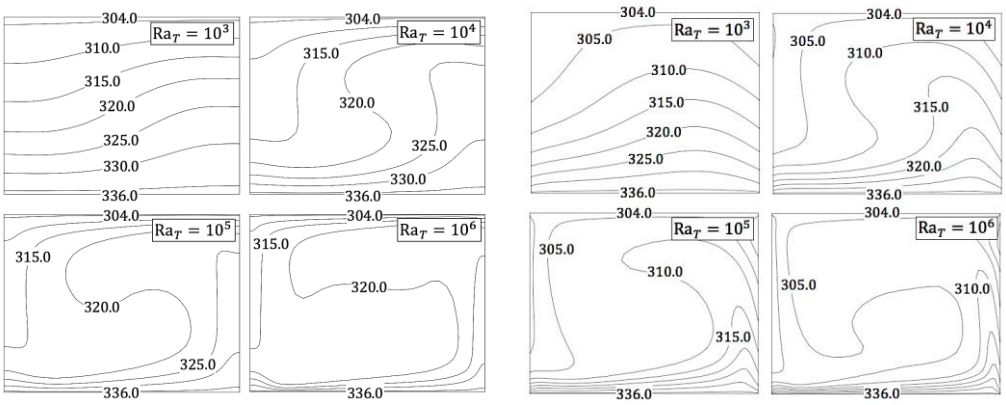

Figure 3. Isotherms for non-radiative case (left) and radiative case (right) for $10^3 \leq Ra_T \leq 10^6$

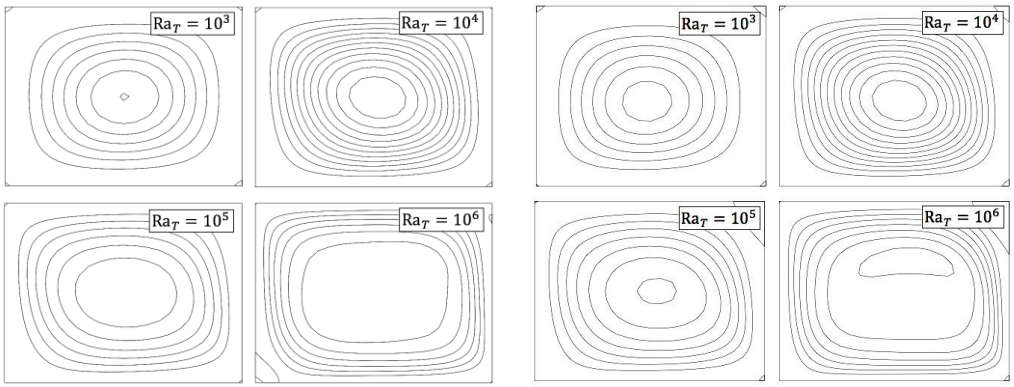

Figure 4. Streamlines for non-radiative case (left) and radiative case (right) for $10^3 \leq Ra_T \leq 10^6$

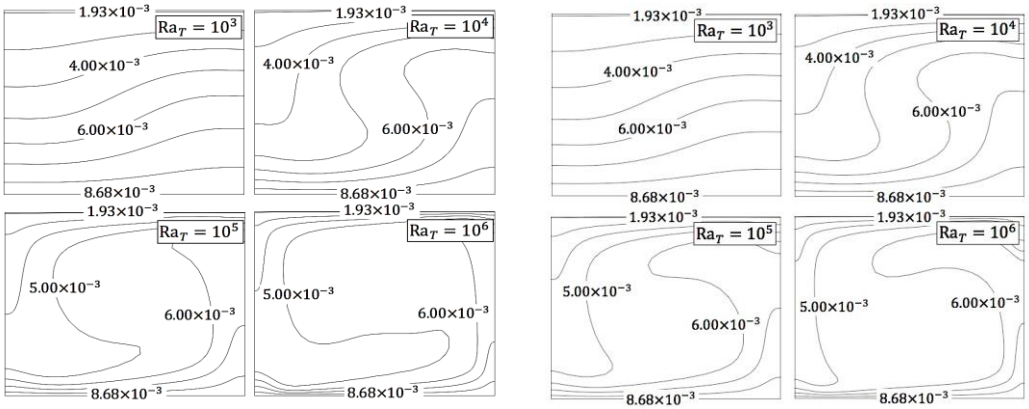

Figure 5. Concentration contour lines for non-radiative case (left) and radiative case (right) for $10^3 \leq Ra_T \leq 10^6$

Table 5 presents comparisons in Nusselt and Sherwood numbers in the solar still cavity for radiative and non-radiative cases. Changes in fluid dynamics profile due to radiation consideration also caused changes in these parameters. Table indicates that convective Nusselt number considerably increased for all thermal Rayleigh values. Radiative Nusselt number increases faster than convective Nusselt number when thermal Rayleigh number increases. Finally, total Nusselt number for radiative case increased considerably.

Table 5: Nusselt and Sherwood numbers comparisons for radiative and non-radiative cases.

	Ra_T (Non-radiative case)				Ra_T (Radiative case)			
	10^3	10^4	10^5	10^6	10^3	10^4	10^5	10^6
Nu	1.180	2.750	4.949	8.715	2.417	4.960	9.227	17.107
Nu_r	-	-	-	-	3.764	8.095	17.436	37.610
Nu_T	1.180	2.750	4.949	8.715	6.181	13.055	26.663	54.717
Sh	1.143	2.602	4.704	8.290	1.127	2.554	4.564	8.071

This effect can be explained due to the fact that isotherms are concentrated at the wall of higher emissivity (bottom wall). Thus, temperature gradient at the hot wall is higher than top wall. The inclusion of radiative term at the energy conservation equation also affected mass transfer. The results presented in Table 5 indicate that Sherwood number along the hot wall decreased slightly.

Figure 6 presents a comparison for local Nusselt number along the solar still hot wall between radiative and non-radiative solar still cavity. This figure shows that local Nusselt number profile changes considerably when comparing both cases. The major difference is close to the walls, where a great Nusselt number value can be found. Walls are surfaces that reflect and emit thermal radiation. Nusselt number is related to buoyancy forces, thus the greatest values are obtained for thermal Rayleigh number equal to 10^6. Figure 7 presents comparison for local Sherwood number for radiative and non-radiative. Sherwood number profile slightly changed for low thermal Rayleigh number. Great change can be seen for

thermal Rayleigh number equal to 10^6, where Sherwood number values increased. Figures 6 and 7 indicate that heat and mass transfer is higher close to left vertical wall. This result agrees with contour lines presented above.

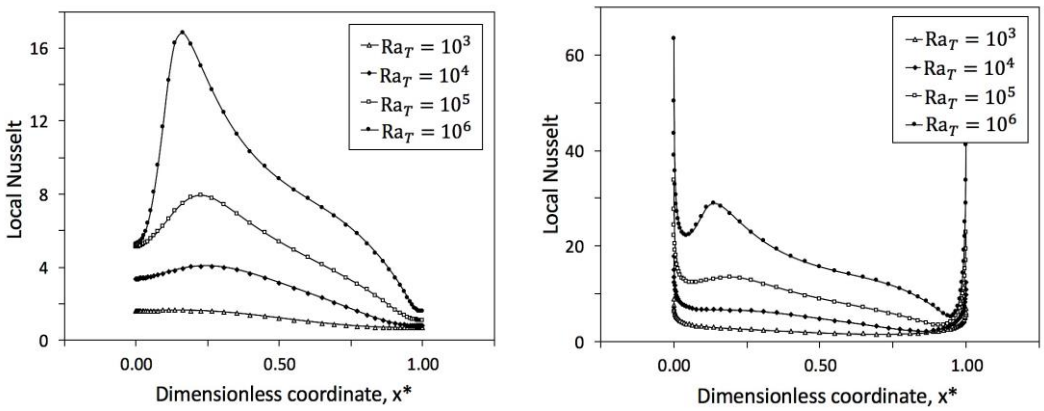

Figure 6. Local Nusselt number along the hot wall for non-radiative (left) and radiative case (right) for $10^3 \leq Ra_T \leq 10^6$

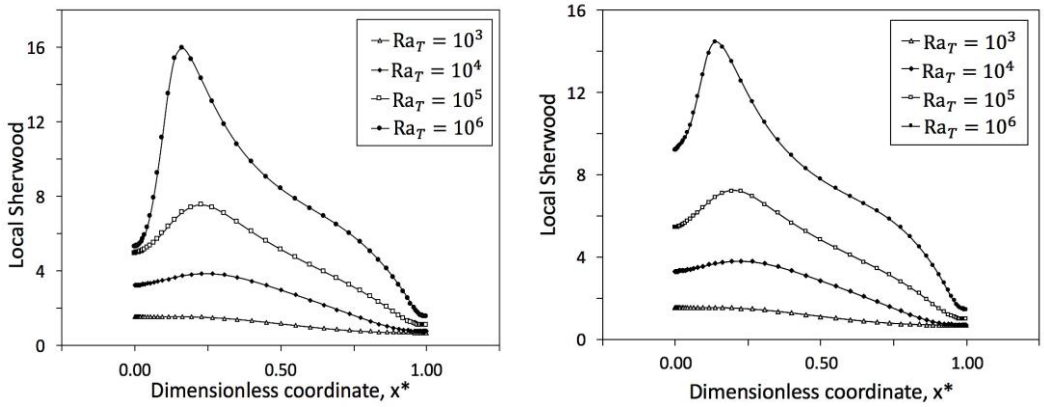

Figure 7. Local Sherwood numbers along the hot wall for non-radiative (left) and radiative case (right) for $10^3 \leq Ra_T \leq 10^6$

5. CONCLUSIONS

Heat transfer and fluid flow by binary natural convection and radiative heat transfer were investigated in a solar still cavity. Conservation equations of mass, momentum and energy equations were discretized through the control volume method and the radiative transfer equation through the discrete ordinates method. Simulations indicate that the consideration of thermal radiation significantly changes heat and mass transfer inside the solar still cavity. Isotherms presented the most prominent changes, for all thermal Rayleigh number values. Isotherms concentrated at the bottom wall due to higher wall emissivity. Streamlines and concentration contour lines also changed, especially for the case where thermal Rayleigh number was high. Nusselt number at the hot wall increased considerably and its profile changed. Sherwood number slightly decreased.

6. ACKNOWLEDGEMENTS

Authors wish to thank CAPES (Coordenação de Aperfeiçoamento de Pessoal de Nível Superior) for graduate scholarship to the first author and CNPQ (Conselho Nacional de Desenvolvimento Científico e Tecnológico) for PQ Research Grant to the second author.

7. REFERENCES

Akiyama, M. and Chong, Q. P., 1997. "Numerical Analysis of Natural Convection with Surface Radiation in a Square Enclosure". *Numerical Heat Transfer*, Vol. 32, p. 419.

Béghein, C., Haghighat, F. and Allard, F., 1992. "Numerical study of double-diffusive natural convection in a square cavity". *International Journal of Heat and Mass Transfer*, Vol. 35, p. 833.

Davis, G.V., 1983. "Natural convection of air in a square cavity: a bench mark numerical solution". *International Journal for Numerical Methods in Fluid*, Vol. 3, p. 249.

Jabrallah, S. B., Belghith, A. and Corriou, J. P., 2002. "Etude des transferts couples de matière et de chaleur dans une cavité rectangulaire: application à une cellule de distillation". *International Journal of Heat and Mass Transfe,* Vol. 45, p. 891.

Lari, K., Baneshi, M., Nassab, S. A. G., Komiya, A. and Maruyama, S., 2011. "Combined Heat Transfer of Radiation and Natural Convection in a Square Cavity Containing Participating Gases". *International Journal of Heat and Mass Transfer*, Vol. 54, p. 5087.

Le Quéré, P., 1991. "Accurate solutions to the square differentially heated cavity at high rayleigh number". *Computer Fluid,* Vol. 20, p. 29.

Modest, M., 2013. *Radiative Heat Transfer*, Academic Press, 3rd edition.

Patankar, S., 1980. *Numerical Heat Transfer and Fluid Flow.* CRC Press.

Paula, A. C. O. and Ismail, K. A. R., 2017. "Analytical modeling and numerical solution of a simple solar still". In *Proceedings of 13th International Conference on Heat Transfer, Fluid Mechanics and Thermodynamics*. Portroz, Slovenia.

Seizai, I. and Mohamad, A., 2000. "Double diffusive convection in a cubic enclosure with opposing temperature and concentration gradient". ", *Physics of Fluid,* Vol. 12, p. 2210.

Sengupta, T. K., Bhaumik, S. and Shameem, U., 2011. "A new compact difference scheme for second derivative in non-uniform grid expressed in self-adjoint form", *Journal of Computational Physics*, Vol. 230, p. 1822.

Sun, Y., Zhang, X. and Howel, J. R., 2017. "Assessment of different radiative transfer equation solvers for combined natural convection and radiation heat transfer problems". *Journal of Quantitative Spectroscopy and Radiative Transfe,* Vol. 194, p. 31.

Weaver, J. A. and Viskanta, R., 1992. "Natural convection in binary gases driven by combined horizontal thermal and vertical solutal gradients". *Experimental Thermal and Fluid Science*, Vol 5, p. 57.

8. RESPONSIBILITY NOTICE

The authors are the only responsible for the printed material included in this paper.